PHYSICAL REVIEW B VOLUME 25, NUMBER 4 15 FEBRUARY 1982

Dynamical aspects of correlation corrections in a covalent crystal

G. Strinati,* H. J. Mattausch, and W. Hanke
Max-Planck-Institut für Festkörperforschung, 7000 Stuttgart 80, Federal Republic of Germany
(Received 11 February 1981)

A central problem in one-electron band calculations is the proper inclusion of exchange and correlations. We have performed a first-principles calculation by utilizing the Green's-function method with an energy-dependent nonlocal self-energy operator obtained by replacing the Coulomb potential in the exchange operator by a dynamically screened interaction. Diamond was chosen as a prototype of covalent materials. To be consistent with a variety of experimental facts, we have taken the dielectric matrix of the medium within the time-dependent screened Hartree-Fock approximation, thereby including both local-field and electron-hole (excitonic) effects. Previous calculations along similar lines have been restricted either to a random-phase-approximation frequency-independent dielectric function or to a plasmon-pole approximation. We have investigated for the first time the role of a realistic frequency and wave-vector-dependent dielectric matrix, and examined the relative importance of the electron-hole excitations and of the plasma resonance across the range of the valence and conduction bands. The correlated band structure was calculated by diagonalizing the quasiparticle equation of motion in a local orbital basis in order to exploit the local character of both the self-energy operator and the orbitals spanning these bands. We have found that the plasma resonance does not contribute appreciably in the energy range about the band gap while it contributes significantly to the valence bandwidth. Our values of 7.4 eV (band gap) and 25.2 eV (valence bandwidth) are in good agreement with reflectivity and photoemission experiments. Implications for the local-density and the energy-independent Coulomb-hole plus screened-exchange approximations are discussed. In addition, our method, by utilizing an energy-dependent self-energy, has also enabled us to calculate quasiparticle damping times (specifically, intraband Auger decay rates) that are consistent with photoemission spectra.

I. INTRODUCTION

The inclusion of many-body effects, such as exchange and correlations, in the calculation of electronic bands of crystals has been an argument of continuous interest over the years. Systematic approaches to this problem have been provided by the Green's-function method[1,2] and by the density-functional formalism.[3,4] The purpose of this paper is twofold. On the one hand, through a pilot calculation on diamond,[5] we aim to draw attention to several features of quasiparticle band calculations in covalent materials that have previously been overlooked or ignored. On the other hand, we try to provide a bridge between the two approaches by making a meaningful comparison of our results, obtained via the Green's-function method, with previous local-density[6] and $X\alpha$ (Ref. 7) calculations on the same material.

The density-functional formalism in its local-density version[3,4] rests its practical utility on a Thomas-Fermi type approximation that holds best for systems, such as metals, with slowly varying electronic density. This approach has indeed become a matter of routine for calculating band structures of metals and has furnished very encouraging results. However, the direct extension to systems with rapidly varying density, such as semiconductors and insulators, is not justified on theoretical grounds and it has also given appreciable departures from experiments, as in the case of diamond and silicon.[6–10] Furthermore, it is well known that the density-functional formalism applies in principle only to the calculation of ground-state properties,[3,4] e.g, the ground-state energy and density. An extension of the ideas of the

local-density approach to deal with excited states properties has been provided by Sham and Kohn,[11] but its application has remained limited.[12]

The Green's-function method has specifically been conceived to deal with excited states properties such as the excitation spectrum of a system (quasiparticles).[1,2] Although this method can be applied to systems with arbitrary density profiles, its main shortcoming is that a detailed knowledge of the screening properties of the medium is required in advance in order to get reasonable quasiparticle properties.

The key quantity in the Green's-function method is the self-energy kernel. In this respect, the usual Hartree-Fock approximation provides a particular approximation for the self-energy [Fig. 1(a)]. However, such an approximation is deficient insofar as it does not include any dynamical relaxation effects of the medium (screening), thereby providing band gaps and bandwidths that are too large compared with the experimental values. Nevertheless, it is customary to take the Hartree-Fock approximation as a "reference level" approximation so that whatever is beyond is generically referred to as "correlations." There are, in fact, reasons to believe that the Hartree-Fock approximation represents a reasonable starting point to include correlation effects.[13,14] This fact is borne out also in model calculations. For instance, the Overhauser plasmon model[15] and the Toyozawa-Kunz polaron model[16–19] are examples of second-order configuration-mixing treatments of correlations[14] where the bare electrons and holes are assumed to interact with a cloud of virtual plasmons and excitons, respectively.

An approximation for the self-energy kernel beyond the Hartree-Fock approximation that has become rather popular is the so-called GW approximation.[20] It consists of replacing the bare Coulomb interaction in the Hartree-Fock approximation by a screened interaction (Fig. 1), thereby taking into account the dynamical rearrangement of the medium as an electron or a hole travels by. This is the approximation that we shall adopt in our calculation of quasiparticle properties in diamond. Previous calculations based on the GW approximation have been restrained by treating the energy dependence of the dielectric matrix in two rather extreme limits, i.e., either as (almost) energy independent or as a delta function peaked at the frequency of a plasmon branch. The first is the so-called Coulomb-hole plus screened-exchange approximation (COHSEX) of Hedin,[20,2] which has been employed by several authors to calculate energy bands of semiconductors and insulators[21–24] in conjunction with other approximations (screening models) to be discussed below. The plasmon-pole approximation, on the other hand, has been mainly applied to metals,[2] but calculations on semiconductors have also been attempted.[25]

This is, in short, the present status of the inclusion of correlations in band calculations. It is apparent that, especially for semiconductors and insulators, the situation is not fully satisfactory. Accordingly, we have endeavored to perform a new calculation that would remedy some of the deficiencies of the previous approaches. Specifically, we have addressed ourselves to the following questions.

(i) The influence of the *energy dependence* of the dieletric matrix on self-energy shifts. The energy range covered by the dielectric matrix is usually partitioned into a low-lying electron-hole continuum and a plasma resonance.[26] In metals the first portion is strongly suppressed by screening for small values of the momentum transfer $\vec{q}$, whereas it dominates for large $\vec{q}$. Combining the two portions into a single-plasmon branch for all values of $\vec{q}$ has then been considered sufficient for calculating self-energy shifts in these materials.[2,15] For nonmetals, however, there has been no detailed investigation of the *relative* importance of the electron-hole excitations versus the plasma resonance across the range of valence and conduction

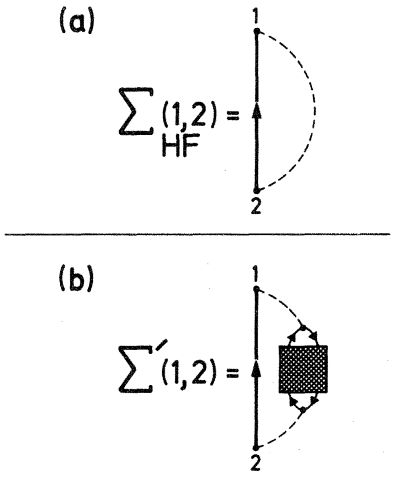

FIG. 1. Graphical representation of the Hartree-Fock (a) and non-Hartree-Fock (b) parts of the GW approximation for the self-energy operator. The shaded box will include bubble and ladder-bubble polarization diagrams (cf. Fig. 1 of Ref. 30).

bands. As we shall see, the energy-independent approximation (COHSEX) that has invariably been used in the past for nonmetals,[21–24] implies that only the electron-hole continuum is in effect retained in the dielectric matrix, but no justification for this procedure has been supplied. Our calculation on diamond will show that, while the sole inclusion of the electron-hole continuum is indeed sufficient to reproduce the band structure in the neighborhood of the band gap, the contribution of the plasma resonance becomes increasingly important as one moves down in the valence bands. We will interpret this result as an indication that, even for nonmetals, a local-density approximation can be appropriate to describe the bands about the gap, whereas it fails for higher excited states.[27]

(ii) The question of the energy dependence of the self-energy is closely related to the choice of the *functional form of the dielectric matrix.* Since these two quantities are functionals of each other, a consistent procedure is required to disentangle them in approximate calculations. In their review paper Hedin and Lundqvist[2] have discussed the use of the GW approximation in conjunction with a random-phase-approximation (RPA) treatment of the screening, regarding this procedure more as an *ansatz* rather than justifying it on the basis of physically plausible criteria. Moreover, in the applications of the GW approximation to nonmetals[21–24] the question of the interconnection between the functional forms of the self-energy and of the dielectric matrix has been hindered by the invariable use of Penn's semiempirical dielectric function.[28] As we shall discuss, the charge conservation criterion is the legitimate candidate to guide the combined choice of the self-energy and of the dielectric matrix. However, as this criterion can only be approximately fulfilled in practical calculations, the internal consistency of a given approximation can ultimately be checked only by comparison with experiments. The inclusion of certain vertex corrections beyond the RPA approximation (the so-called ladder-bubble diagrams) has been shown by Hanke and Sham[29–32] to be essential and sufficient for a quantitative account of the optical response in covalent materials. Quite generally, we make detailed use of this earlier work on the many-body effects in the optical spectra, in particular diamond,[29,30] which resulted in quantitative agreement with the experimental data. It is our guideline for choosing approximations on the screening part of the self-energy employing the same wave functions, energies, overlap assumptions, etc., and many-body corrections. In this paper we will verify that the inclusion of the same kind of vertex corrections is required in order to obtain values for the band gap and the valence bandwidth that are consistent with the experimental values.

(iii) *Lifetimes* of quasiparticle excited states can be calculated only when the approximation for the self-energy kernel is energy dependent.[33] Especially for materials like diamond with a wide valence bandwidth, such an investigation may be of some theoretical interest on its own and may also serve to stimulate comparison with photoemission data. Our approach will enable us to produce for the first time the energy-dependent intraband Auger decay time of a valence hole in diamond.

The plan of the paper is as follows. The theoretical framework is presented in Sec. II, the details of the calculation for diamond are given in Sec. III, and the results are discussed in Sec. IV. Section V contains our conclusions.

II. THEORETICAL FRAMEWORK

In this section we comment on the coupled set of integral equations defining the self-energy operator and present a truncation procedure (or decoupling) of this set of equations which is suggested by charge conservation criteria. We discuss also properties of the self-energy operator that are relevant to our purposes, namely, the symmetries under space-group operations and under interchange of the position variables, and the short-range property. By utilizing an expansion into localized orbitals, we then cast the quasiparticle equation of motion in a form that is particularly suited to the study of semiconductors and insulators. Finally, we review briefly the theory of the dielectric response in insulators. To keep our presentation reasonably selfcontained, some material other than ours will be included.

A. Beyond the Hartree-Fock approximation: The link between the self-energy operator and the dielectric matrix

Quasielectrons and quasiholes signify approximate excited states of the $(N+1)$ particle and $(N-1)$ particle system, respectively. Their excitation energies (measured from the N particle ground-state energy) and the corresponding energy

spreads (which are related to the lifetimes of the approximate excited states) can be obtained by locating the singularities of the one-electron Green's function in the complex energy plane.[34] For a crystalline system this manifold of states can be organized into a many-body (or correlated) band structure that generalizes the ordinary independent-particle band picture.

The exact expression of the one-electron Green's function for a system of interacting particles is, of course, not known since it would imply a complete knowledge of the many-body ground and excited states. Conventional perturbative treatments[1] cannot be applied in a realistic many-body problem owing to convergence difficulties.[35] A nonperturbative approach is provided by the density-functional formalism, but has so far only been considered in connection with the local-density approximation.[11,12] Another, in principle, nonperturbative approach is provided by the functional-derivative formalism (see, for example, Refs. 2 and 20). A central role in this approach is played by the *self-energy* operator $\Sigma(\vec{r}, \vec{r}'; E)$ from whose knowledge the excitation energies E_i of the quasiparticle states can be obtained by solving the equation

$$[H_{\rm av}(\vec{r})-E_i]\phi_i(\vec{r}) + \int d\vec{r}'\Sigma(\vec{r}, \vec{r}'; E_i)\phi_i(\vec{r}')=0 . \tag{2.1}$$

Here $H_{\rm av}(\vec{r})$ is an average (Hartree) local Hamiltonian that includes the Coulomb effect both of the nuclei and of the average electronic charge distribution in the ground state, $\langle n(\vec{r})\rangle$:

$$H_{\rm av}(\vec{r})=-\frac{\hbar^2}{2m}\vec{\nabla}^2-\sum_n Z_n v(\vec{r}-\vec{R}_n) + \int dr' v(\vec{r}-\vec{r}')\langle n(\vec{r}')\rangle , \tag{2.2}$$

where we have set $v(\vec{r}-\vec{r}')=e^2/|\vec{r}-\vec{r}'|$.[36]

As for the Green's function, the exact form of the self-energy kernel is not explicitly known. Yet one can derive a set of coupled integral equations connecting the *exact* self-energy to the exact Green's function (G), the irreducible polarizability ($\tilde{\chi}$), the vertex function (Γ), and the dynamically screened interaction (W) (Ref. 37):

$$\Sigma(12)=i\hbar\int d34W(1^+3)G(14)\Gamma(42,3) , \tag{2.3a}$$

$$W(12)=v(12)+\int d34v(13)\tilde{\chi}(34)W(42) , \tag{2.3b}$$

$$\tilde{\chi}(12)=-i\hbar\int d34G(23)G(42)\Gamma(34,1) , \tag{2.3c}$$

$$\Gamma(12,3)=\delta(12)\delta(13) + \int d4567\frac{\delta\Sigma(12)}{\delta G(45)}G(46)G(75)\Gamma(67,3) . \tag{2.3d}$$

In Eqs. (2.3) the labels 1,2,... stand for the set of position, spin, and time variables, while 1^+ implies that the time variable t_1 is augmented by a positive infinitesimal. These equations explicitly show how the self-energy Σ depends on the dielectric matrix $\epsilon=1-v\tilde{\chi}$ through the vertex function Γ and how Γ, in turn, depends on Σ. This is precisely what we meant in the introduction for interconnection between Σ and ϵ.

In any practical calculation there arises the question of how to *truncate* the set of coupled equations (2.3). Common practice has been to make specific *ansatz* on the functional forms of Σ and Γ *separately*. A popular choice for Σ has been the use of the so-called GW approximation,[2,20] where one sets

$$\Sigma(12)=i\hbar W(1^+2)G(12) , \tag{2.4}$$

while the screening properties of the medium entering W were treated within the random-phase approximation (RPA) by setting

$$\Gamma(12,3)=\delta(12)\delta(13) . \tag{2.5}$$

No criterion, however, has been supplied to justify this specific decoupling of the set of equations (2.3). We notice in passing that the familiar Hartree-Fock approximation for Σ reappears as a particular limit of Eq. (2.4) when one replaces the dynamically-screened interaction W by the bare instantaneous Coulomb potential v. In fact, one may sort out the Hartree-Fock from the GW approximation by splitting the expression (2.4) in terms of $\Sigma_{\rm HF}$ and of a remainder Σ':

$$\Sigma(12)=\Sigma_{\rm HF}(12)+\Sigma'(12) . \tag{2.6}$$

The two terms in Eq. (2.6) are represented graphically in Figs. 1(a) and 1(b), respectively. It is obvious that within the Hartree-Fock approximation for Σ the question of the corresponding choice of Γ does not arise.

Criteria to justify a particular choice for Σ and Γ cannot emerge from Eqs. (2.3) themselves but should rather be imposed as external constraints, exploiting, for instance, special symmetries of the system. In particular, the invariance of the theory under local gauge transformations of the first and

second kind (which is related to current conservation)[38] provides an explicit interconnection between Σ and Γ in the sense that the following identity is satisfied:

$$\frac{i}{\hbar}(t_1-t_2)\Sigma(12)=\delta(12)-\int d3\Gamma(12,3)$$
$$\equiv-\int d3\Lambda(12,3)\ . \tag{2.7}$$

An identity of this kind is known in quantum electrodynamics as the Ward-Takahashi identity.[39]

In order to gain insight in Eq. (2.7) in the present context, we recall that in the derivation of Eqs. (2.3) the system of N interacting nonrelativistic particles is coupled to a time-dependent weak external scalar potential which at the end is allowed to vanish. We can then take advantage of the freedom in the choice of this potential and vary it by a constant infinitesimal amount $-\alpha$ by introducing a particular class of gauge functions

$$F(\vec{r},t)=\alpha ct\ , \tag{2.8}$$

c being the velocity of light. To preserve gauge invariance, the field operators must at the same time be multiplied by $\exp(ie\alpha t/\hbar)$, thereby inducing the Green's function to vary by the amount[40]

$$\delta G(12)=\frac{i}{\hbar}e\alpha(t_1-t_2)G(12)\ . \tag{2.9}$$

The corresponding variation of the inverse Green's function can be expressed in terms of the self-energy as

$$\delta G^{-1}(12)=e\alpha\left[\delta(12)-\frac{i}{\hbar}(t_1-t_2)\Sigma(12)\right]\ . \tag{2.10}$$

On the other hand, from the original definition of the vertex function[2] one may also state that, under the infinitesimal gauge transformation generated by the function (2.8),

$$\delta G^{-1}(12)=e\alpha\int d3\,\Gamma(12,3)\ . \tag{2.11}$$

Comparison of Eqs. (2.10) and (2.11) leads to Eq. (2.7).

To investigate the implications of Eq. (2.7) it is convenient to take its time Fourier transform, which reads

$$\frac{1}{\hbar}\frac{\partial}{\partial\omega}\Sigma(\vec{r},\vec{r}';\omega)=-\int d\vec{r}''\Lambda(\vec{r},\vec{r}';\vec{r}''\,|\,\omega,\omega)\ . \tag{2.12}$$

We stress that this relation is but an identity between the *exact* Σ and Λ. In approximation methods used in finding *approximate* solutions, however, Eq. (2.12) provides a criterion to make the choices of Σ and Λ, although in practice one might not be able to fulfill Eq. (2.12) exactly. Consider, in particular, the GW approximation for Σ, Eq. (2.4). Utilizing a formal expansion in terms of the bare Coulomb potential v and of the Hartree Green's function G_0 (that corresponds to the approximation $\Sigma=0$) one may verify that, to satisfy Eq. (2.12), it is sufficient to take the vertex function Γ as the solution of the integral equation (2.3d) with Σ given by Eq. (2.4). This approximation for Γ contains three kinds of terms: (i) the RPA term (2.5) that does not include any vertex correction, (ii) the ladder diagrams corresponding to the time-dependent screened Hartree-Fock approximation (TDSHF),[29–32] which are obtained by retaining only the functional derivative of the explicit G in Eq. (2.4), and (iii) other terms which are obtained by taking into account also the dependence of the screened interaction on G. Inclusion of the last class of terms constitutes a rather formidable task that exceeds our purposes. In our calculation we will limit ourselves to the GW approximation for Σ and also consider the RPA and the TDSHF approximation for screening W only, postponing any comment on the validity of either approximation to comparison with experiments.

We note at this point that, in the TDSHF approximation, the potential entering the ladder diagrams for Γ should itself be the fully screened potential W, the process repeating itself in an open-ended way. In our calculation we have truncated this process by approximating the potential in Γ (i.e., the screening of the electron-hole interaction) by a static screened potential calculated from a phenomenological dielectric function. As pointed out before, this choice as well as the general strategy of implementing many-body effects in the screening entering Σ, is justified on pragmatic grounds. Previous detailed studies of optical response in covalent crystals, including diamond, achieved quantitative agreement with experimental data[29–32] using precisely the approximations discussed above (TDSHF).

A few words of comment on the choice of the GW approximation for Σ are also worthy. This approximation undoubtedly represents an important improvement over the Hartree-Fock approximation since it includes the dynamical polarization of the medium. Yet it leaves out several other

correlation effects that might turn out to be dominant in some cases.[41] In particular, one might expect the GW approximation to break down in the case of narrow valence bands, as for LiF,[19,24] or in the case of core levels, where it might not be appropriate to treat the screening of the sole valence electrons around a localized hole within the linear response approximation.[42] By the same token, one may hope that the GW approximation is sufficient to describe wide valence bands, as in the case of diamond. This expectation will indeed be fulfilled by our calculation. Finally, going beyond the GW approximation will make it harder to satisfy the current conservation criterion, Eq. (2.12), even approximately.

B. Properties of the self-energy operator

In order to cast the quasiparticle equation (2.1) in a form suitable for numerical solution, we make use of the following properties of the self-energy operator.

(i) The Hartree Hamiltonian (2.2) is *invariant* under the replacement $\vec{r}\rightarrow\{R|\vec{w}\}\vec{r}=R\vec{r}+\vec{w}$, $\{R|\vec{w}\}$ being an operation of the space group of the crystal. Similarly, one can show for the full self-energy[43]

$$\Sigma(\{R\mid\vec{w}\}\vec{r},\{R\mid\vec{w}\}\vec{r}';E)=\Sigma(\vec{r},\vec{r}';E)\ . \tag{2.13}$$

This property can be established first proving the analogous property for the Green's function G by exploiting the structure of its spectral representation, and then utilizing the functional relation between G and Σ given by Dyson's equation. Equation (2.13) can also be explicitly verified within the approximation we have adopted for Σ, Eq. (2.4), by recalling the symmetry properties of the dielectric matrix.[44]

Equation (2.13), when specialized to the subset of operations belonging to the translational subgroup of the crystal, implies that the wave functions $\phi_i(\vec{r})$ in Eq. (2.1) can be chosen to satisfy the Bloch condition. The label i will thus stand for the pair $(n,\vec{k})$, where the wave vector $\vec{k}$ is confined to the Brillouin zone and n is a band index.

(ii) The self-energy operator is *symmetric* under the interchange of $\vec{r}$ and $\vec{r}'$, that is

$$\Sigma(\vec{r},\vec{r}';E)=\Sigma(\vec{r}',\vec{r};E)\ . \tag{2.14}$$

Equation (2.14) (that holds in the absence of magnetic fields) can be proven in general following the same steps indicated at (i), and can again be explicitly verified for the GW approximation.

(iii) The self-energy is a *short-range* kernel in $|\vec{r}-\vec{r}'|$. This property has been proven by Sham and Kohn on the basis of general graphical considerations,[11] and has been checked numerically by Hedin in his work on the electron gas.[20] The short-range property implies that, when viewed as a matrix in the continuous indices $\vec{r}$ and $\vec{r}'$, $\Sigma(\vec{r},\vec{r}';E)$ will have matrix elements appreciably different from zero only in a neighborhood of the diagonal, $\vec{r}=\vec{r}'$.

C. The quasiparticle equation in local orbital representation

For a homogeneous system, such as an electron gas in jellium, symmetry arguments alone enable us to solve Eq. (2.1) directly. In this case, in fact, $\Sigma(\vec{r},\vec{r}';E)=\Sigma(\vec{r}-\vec{r}';E)$, so that the wave functions $\phi_i(\vec{r})$ are plane waves of wave vector $\vec{k}$ and the corresponding eigenvalues are $E(\vec{k})=\vec{k}^2+\Sigma(\vec{k};E(\vec{k}))$. In contrast, our efforts in this paper are focused on physical systems, like covalent materials, where the electron gas limit cannot be applied owing to the strong modulation of the periodic part of the Bloch functions. In this case it seems most appropriate to express the Bloch functions in terms of a set of orbitals $\Phi_\nu(\vec{r}-\vec{l})$ that are localized about the lattice sites $\vec{l}$:

$$\phi_{n\vec{k}}(\vec{r})=\sum_{\{\nu\}}\left[\mathcal{N}^{-1/2}\sum_{\vec{l}}e^{i\vec{k}\cdot\vec{l}}\Phi_\nu(\vec{r}-\vec{l})\right]c_{\nu n}(\vec{k})\ , \tag{2.15}$$

$\mathcal{N}$ being the number of lattice sites. The number of indices $\{\nu\}$ equals the number of bands that are in contact with each other but are isolated from other bands.[45]

The quasiparticle equation (2.1) can now be reduced to an algebraic eigenvalue problem for the coefficients $c_{\nu n}(\vec{k})$ of the expansion (2.15) by inserting Eq. (2.15) into Eq. (2.1) and projecting onto alternative $\Phi_\nu(\vec{r})$. At any given $\vec{k}$ in the Brillouin zone (BZ) one then has to solve

$$\sum_{\{\nu'\}} [\langle \nu \mid \epsilon(\vec{k}) \mid \nu' \rangle + \langle \nu \mid \Sigma(\vec{k}; E_n(\vec{k})) \mid \nu' \rangle] c_{\nu' n}(\vec{k}) = E_n(\vec{k}) c_{\nu n}(\vec{k}) \ . \tag{2.16}$$

We have introduced the notation

$$\langle \nu \mid \epsilon(\vec{k}) \mid \nu' \rangle = \sum_{\vec{l}} e^{i\vec{k}\cdot\vec{l}} \langle \Phi_\nu(\vec{r}) \mid H_{\rm av}(\vec{r}) \mid \Phi_{\nu'}(\vec{r} - \vec{l}) \rangle \tag{2.17}$$

and

$$\langle \nu \mid \Sigma(\vec{k}; E) \mid \nu' \rangle = \sum_{\vec{l}} e^{i\vec{k}\cdot\vec{l}} \langle \Phi_\nu(\vec{r}) \mid \Sigma(\vec{r}, \vec{r}'; E) \mid \Phi_{\nu'}(\vec{r}' - \vec{l}) \rangle \ . \tag{2.18}$$

Owing both to the short-range property of the self-energy operator and to the localization of the orbitals $\Phi_\nu(\vec{r})$, we expect the summation over $\vec{l}$ in Eq. (2.18) to extend up to a few shells of lattice vectors about $\vec{l}=0$, akin to the summation in Eq. (2.17).[46] The explicit form of the local orbitals $\Phi_\nu(\vec{r})$ will be discussed in Sec. III.

We notice that, at any given $\vec{k}$ in the Brillouin zone, the eigenvalues $E_n(\vec{k})$ of Eq. (2.16) have to be determined through a self-consistent loop since they also appear as argument of the self-energy operator. In addition, we recall that the matrix $\langle \nu | \Sigma(\vec{k}; E) | \nu' \rangle$ is in general *non-Hermitian.* In fact, one may verify using the symmetry properties (2.13) and (2.14) that the real and imaginary part of the self-energy operator yield the Hermitian and skew-Hermitian part of the matrix $\langle \nu | \Sigma(\vec{k}; E) | \nu' \rangle$, respectively. This implies that the eigenvalues $E_n(\vec{k})$ of Eq. (2.16) are in general complex, the real part furnishing the excitation energy of an approximate eigenstate of the $(N \pm 1)$ electron system and the imaginary part providing the corresponding energy spread. In the particular case when Σ is assumed to be energy independent, as in the Hartree-Fock and in the COHSEX approximation, the matrix (2.18) becomes Hermitian, thereby preventing the calculation of the lifetimes of the quasiparticle states.[33]

To calculate the matrix elements (2.18) we start by taking the time Fourier transform of the GW expression for Σ, Eq. (2.4),

$$\Sigma(\vec{r}, \vec{r}'; E) = \frac{i}{2\pi} \int_{-\infty}^{+\infty} dE' e^{iE'\delta} G(\vec{r}, \vec{r}'; E + E') \times W(\vec{r}, \vec{r}'; E') \ , \tag{2.19}$$

where δ is a positive infinitesimal needed to ensure convergence of the Hartree-Fock term. Equation (2.19) acquires the usual form of a convolution integral when recalling that W is an even function of the frequency. The Green's function that appears in Eq. (2.19) *(also* through the screened interaction W) should, in principle, be the full self-consistent Green's function obtained by solving Dyson's equation with Σ given by Eq. (2.19) itself. In actual calculations one starts by approximating G by the expression

$$G(\vec{r}, \vec{r}'; E) = \sum_n \sum_{\vec{k}}^{\rm BZ} \frac{\phi_{n\vec{k}}(\vec{r}) \phi_{n\vec{k}}(\vec{r}')^*}{E - E_n(\vec{k}) + i\eta \, \mathrm{sgn}[E_n(\vec{k}) - E_F]} \ , \tag{2.20}$$

where $\eta \to 0+$ and the Fermi level E_F is placed somewhere within the gap. The Bloch functions $\phi_{n\vec{k}}(\vec{r})$ and the corresponding band eigenvalues $E_n(\vec{k})$ in Eq. (2.20) are borrowed from a preliminary calculation (i.e., $X\alpha$ or local density) that includes exchange and correlations in an approximate way. Once the new band structure is obtained by solving Eq. (2.1), the calculation should be repeated, using again for G an approximate expression of the type (2.20), until self-consistency is attained. We have not aimed, however, to achieve this kind of self-consistency in our calculation for diamond where we have assumed G of the form (2.20) with the bands taken from a previous $X\alpha$ calculation.[7]

The Green's function (2.20) can also be expressed in a local orbital basis by utilizing the expansion (2.15). We get

$$G(\vec{r}, \vec{r}'; E) = \sum_{\{\sigma\sigma'\}} \sum_{\vec{s}\,\vec{s}'} \Phi_\sigma(\vec{r} - \vec{s}) G_{\sigma\sigma'}(\vec{s} - \vec{s}'; E) \Phi^*_{\sigma'}(\vec{r}' - \vec{s}') \ , \tag{2.21}$$

where the matrix elements $G_{\sigma\sigma'}(\vec{m};E)$ are given by

$$G_{\sigma\sigma'}(\vec{m};E)=\sum_n \frac{1}{\mathcal{N}} \sum_{\vec{k}}^{BZ} \frac{c_{\sigma n}(\vec{k})e^{i\vec{k}\cdot\vec{m}}c_{\sigma' n}(\vec{k})^*}{E-E_n(\vec{k})+i\eta\,\mathrm{sgn}[E_n(\vec{k})-E_F]} . \tag{2.22}$$

It is clear that what is still needed to calculate the matrix (2.18) explicitly are the matrix elements of the screened interaction $W(\vec{r},\vec{r}';E)$ between pairs of local orbitals. To this end, we should first find a suitable expression for W.

D. RPA and TDSHF treatment of the screening in local orbital representation

A closed-form expression for $W(\vec{r},\vec{r}';E)$ can be obtained by solving formally the integral equation (2.3b) and then taking the time Fourier transform of its solution:

$$W(\vec{r},\vec{r}';E)=v(\vec{r}-\vec{r}')+\int d\vec{r}_1 d\vec{r}_2 v(\vec{r}-\vec{r}_1)\chi_T(\vec{r}_1,\vec{r}_2;E)v(\vec{r}_2-\vec{r}')\equiv v(\vec{r}-\vec{r}')+W'(\vec{r},\vec{r}';E) . \tag{2.23}$$

We have here introduced the (time-ordered) polarization χ_T and we have sorted out from W the bare Coulomb interaction v. The two terms on the right-hand side of Eq. (2.23) correspond to Σ_{HF} and Σ' of Eq. (2.6), respectively.

Notice that writing Eq. (2.23) assumes both (i) that the integral equation (2.3d) for Γ has been solved and the corresponding solution inserted into Eq. (2.3c) to obtain the irreducible polarizability $\tilde{\chi}$, and (ii) that the integral equation (2.3b) for W has also been solved. Step (i) is straightforward within the RPA approximation where Γ is given by Eq. (2.5), but becomes already nontrivial in the TDSHF approximation. However, it has been shown by Hanke and Sham in the context of the linear response theory[30] that the inclusion of the ladder diagrams for Γ becomes feasible when using a local orbital representation similar to Eq. (2.15) to express the Bloch functions of the valence and conduction bands that are coupled in the screening process. By the same token, they also showed that step (ii), which involves the inversion of the dielectric matrix since $\chi=\tilde{\chi}\epsilon^{-1}$, can be readily performed using a local orbital representation. The result is that the (retarded) polarization matrix acquires the following form:

$$\chi_R(\vec{r},\vec{r}';E)=\frac{1}{V}\sum_{\vec{q}}^{BZ}\sum_{\vec{G}\vec{G}'} e^{i(\vec{q}+\vec{G})\cdot\vec{r}}\chi_R(\vec{q}+\vec{G},\vec{q}+\vec{G}';E)e^{-i(\vec{q}+\vec{G}')\cdot\vec{r}'} , \tag{2.24}$$

where

$$\chi_R(\vec{q}+\vec{G},\vec{q}+\vec{G}';E)=\frac{1}{\Omega_0}\sum_{\vec{l}\nu\mu}\sum_{\vec{l}'\nu'\mu'} A_{\vec{l}\nu\mu}(\vec{q}+\vec{G})S_{\vec{l}\nu\mu,\vec{l}'\nu'\mu'}(\vec{q};E)A^*_{\vec{l}'\nu'\mu'}(\vec{q}+\vec{G}') . \tag{2.25}$$

In Eqs. (2.24) and (2.25) $\vec{q}$ is a wave vector confined to the Brillouin zone $\vec{G}$ and $\vec{G}'$ are vectors of the reciprocal lattice, and Ω_0 is the volume of the Wigner-Seitz cell ($V=\mathcal{N}\Omega_0$). The A's in Eq. (2.25) are given by:

$$A_{\vec{l}\nu\mu}(\vec{q}+\vec{G})=\int d\vec{r}\,\Phi^*_\nu(\vec{r})e^{-i(\vec{q}+\vec{G})\cdot\vec{r}}\Phi_\mu(\vec{r}-\vec{l}) , \tag{2.26}$$

and the screening matrix $S(\vec{q};E)$ is given by (in matrix notation):

$$S(\vec{q};E)=N(\vec{q};E)\{1-[V(\vec{q})-\tfrac{1}{2}V^x(\vec{q})]N(\vec{q};E)\}^{-1} . \tag{2.27}$$

Here we note the following.

(i) $N(\vec{q};E)$ is the RPA irreducible polarizability in local orbital representation:

$$N_{\vec{l}\nu\mu,\vec{l}'\nu'\mu'}(\vec{q};E)=\frac{1}{\mathcal{N}}\sum_{\vec{k}}^{BZ} e^{i(\vec{k}+\vec{q})\cdot(\vec{l}-\vec{l}')} \times \sum_{n_1 n_2} c^*_{\nu n_2}(\vec{k})c_{\mu n_1}(\vec{k}+\vec{q})\frac{2[f_{n_1}(\vec{k}+\vec{q})-f_{n_2}(\vec{k})]}{E_{n_1}(\vec{k}+\vec{q})-E_{n_2}(\vec{k})-E-i\eta}c_{\nu' n_2}(\vec{k})c^*_{\mu' n_1}(\vec{k}+\vec{q}) \tag{2.28}$$

($\eta\to 0+$), $f_n(\vec{k})$ being the occupation number of the state $n\vec{k}$. Note that the band eigenvalues and the Bloch functions [represented by the coefficients $c_{\nu n}(\vec{k})$] entering Eq. (2.28) are the same as those utilized in the expression (2.20) for the Green's function.

(ii) $V(\vec{q})$ is the Fourier transform of the matrix of the bare Coulomb potential between pairs of local orbitals:

$$V_{\vec{l}\nu\mu,\vec{l}'\nu'\mu'}(\vec{q})=\sum_{\vec{m}} e^{-i\vec{q}\cdot\vec{m}}\langle\Phi^*_\nu(\vec{r}-\vec{m})\Phi_\mu(\vec{r}-\vec{l}-\vec{m})\,|\,v(\vec{r}-\vec{r}')\,|\,\Phi^*_{\nu'}(\vec{r}')\Phi_{\mu'}(\vec{r}'-\vec{l}')\rangle \tag{2.29}$$

$$=\frac{1}{\Omega_0}\sum_{\vec{G}} A^*_{\vec{l}\nu\mu}(\vec{q}+\vec{G})v(\vec{q}+\vec{G})A_{\vec{l}'\nu'\mu'}(\vec{q}+\vec{G})$$

[$v(\vec{q}+\vec{G})=8\pi/|\vec{q}+\vec{G}|^2$], and $V^x(\vec{q})$ is its screened exchange counterpart:

$$V^x_{\vec{l}\nu\mu,\vec{l}'\nu'\mu'}(\vec{q})=\sum_{\vec{m}} e^{-i\vec{q}\cdot\vec{m}}\langle\Phi^*_\nu(\vec{r}'-\vec{m})\Phi_\mu(\vec{r}-\vec{l}-\vec{m})\,|\,v_s(\vec{r}-\vec{r}')\,|\,\Phi^*_{\nu'}(\vec{r}')\Phi_{\mu'}(\vec{r}-\vec{l}')\rangle\ . \tag{2.30}$$

As discussed in Sec. II A, the potential v_s in Eq. (2.30) is a static approximation to the full screened potential W. Its explicit form will be considered in Sec. III C. We only remark here that screening the Coulomb potential in the exchange integral was found essential for getting meaningful values for the optical constants, in particular for the static dielectric constant. Note also that the RPA approximation for the screening matrix $S(\vec{q};E)$ can be simply obtained from the TDSHF expression (2.27) by setting $V^x(\vec{q})=0$, and that in both the RPA and the TDSHF forms the so-called local-field effects (i.e., the off-diagonal terms in $\vec{G}$ and $\vec{G}'$) are automatically included.

To obtain the time-ordered polarization matrix $\chi_T(\vec{r},\vec{r}';E)$, which is needed in the expression (2.23) of the dynamically screened interaction, from the retarded polarization matrix of Eqs. (2.24)–(2.30) one has to recall that the two functions are related by the prescription[2]

$$\chi_T(\vec{r},\vec{r}';E)=[\Theta(E)+\Theta(-E)K]\chi_R(\vec{r},\vec{r}';E) \tag{2.31}$$

for real E, where $\Theta(E)$ is the unit step function and K is the complex-conjugation operator.

The matrix elements

$$\langle\Phi_\nu(\vec{r})\,|\,\Sigma(\vec{r},\vec{r}';E)\,|\,\Phi_{\nu'}(\vec{r}'-\vec{l})\rangle$$

of Eq. (2.18) which are needed to solve the quasiparticle equation (2.16) can now be expressed in terms of the screening matrix (2.27) and of the Coulomb matrix (2.29). In particular, we need to obtain an explicit expression only for the matrix elements of $\Sigma'(\vec{r},\vec{r}';E)$ [cf. Eq. (2.6)] because we can get the Hartree-Fock matrix elements from a separate procedure (Sec. III A). We start by restricting the range of the integration in Eq. (2.19) to the positive real energy axis where, according to Eq. (2.31), χ_T and χ_R coincide. This can be done by recalling that χ_T is an even function of E and replacing $G(\vec{r},\vec{r}';E+E')$ by

$$\bar{G}(\vec{r},\vec{r}';E,E')=G(\vec{r},\vec{r}';E+E') +G(\vec{r},\vec{r}';E-E')\ . \tag{2.32}$$

Moreover, the convergence factor $\exp(iE'\delta)$ can now be dropped from the integration over E' since one can show that $\chi_R(\vec{r},\vec{r}';E')=O(E'^{-2})$ for large E'. Inserting the expression (2.24) for χ_R into the second term on the right-hand side of Eq. (2.23) and entering the resulting expression together with the expansion (2.21) for the Green's function into the convolution integral for $\Sigma'(\vec{r},\vec{r}';E)$, we get after some rearrangements

$$\langle \Phi_\tau(\vec{r}) \mid \Sigma'(\vec{r},\vec{r}';E) \mid \Phi_{\tau'}(\vec{r}'-\vec{t}) \rangle = \frac{i}{2\pi} \int_0^\infty dE' \sum_{\{\sigma\sigma'\}} \sum_{\vec{m}\,\vec{m}'} \bar{G}_{\sigma\sigma'}(-\vec{m};E,E') \frac{1}{\mathcal{N}} \sum_{\vec{q}}^{BZ} e^{-i\vec{q}\cdot\vec{m}} W'_{\vec{m}'+\vec{m}\,\sigma\tau,\,\vec{m}'+\vec{t}\,\sigma'\tau'}(\vec{q};E') \,. \tag{2.33}$$

Here

$$W_{\vec{m}\,\sigma\tau,\,\vec{m}'\sigma'\tau'}(\vec{q};E) = \sum_{\vec{l}\,\nu\mu} \sum_{\vec{l}'\nu'\mu'} V_{\vec{m}\,\sigma\tau,\,\vec{l}\,\nu\mu}(\vec{q}) S_{\vec{l}\,\nu\mu,\,\vec{l}'\nu'\mu'}(\vec{q};E) V_{\vec{l}'\nu'\mu',\,\vec{m}'\sigma'\tau'}(\vec{q}) \tag{2.34}$$

is the Fourier transform of the matrix of the potential $W'(\vec{r},\vec{r}';E)$ between pairs of local orbitals. The expression (2.34) is particularly attractive since $W'(\vec{q};E)$ is obtained by a simple matrix multiplication of the Coulomb matrix with the screening matrix. Evaluation of the matrix elements (2.33) constitutes the main numerical effort of this work.

III. NUMERICAL CALCULATION

A. The Hartree-Fock band structure

The excitation energies $E_n(\vec{k})$ of the quasiparticle states are obtained as the (complex) eigenvalues of the matrix $\langle \nu \mid \epsilon(\vec{k}) \mid \nu' \rangle + \langle \nu \mid \Sigma(\vec{k};E) \mid \nu' \rangle$ defined by Eqs. (2.17) and (2.18). Within the GW approximation for the self-energy operator, we have split up the matrix elements $\langle \nu \mid \epsilon(\vec{k}) \mid \nu' \rangle + \langle \nu \mid \Sigma(\vec{k};E) \mid \nu' \rangle$ into an energy-independent Hartree-Fock part $\langle \nu \mid \epsilon(\vec{k}) \mid \nu' \rangle + \langle \nu \mid \Sigma_{HF}(\vec{k}) \mid \nu' \rangle$ and an energy-dependent remainder $\langle \nu \mid \Sigma'(\vec{k};E) \mid \nu' \rangle$. We shall determine the Hartree-Fock part by making a Slater-Koster fit to an existing Hartree-Fock band calculation, while the remainder will be determined by evaluating the matrix elements (2.33) explicitly. This procedure is, however, not completely rigorous because the one-particle density matrix $\rho(\vec{r},\vec{r}')$ that appears in the Hartree-Fock matrix elements should in principle be recalculated as correlations are added. We then justify neglecting this change in $\rho(\vec{r},\vec{r}')$ by invoking Brillouin's theorem[13] which states that the mean value of any one-particle operator is stationary to first order under correlation corrections.

Diamond was chosen as a prototype of covalent materials. There were several reasons for this choice, namely, the availability of accurate Hartree-Fock calculations for this light core material, the appropriateness of a local orbital description for the valence and conduction bands (in particular, for describing the screening properties), the possibility of studying the effects of the energy-dependence of the self-energy operator owing to the large valence bandwidth, and the resemblance to the covalent semiconductors.

Equation (2.16) was then decoupled into two disjoint 4×4 matrix equations for the two sets of valence and conduction bands by taking the local orbitals $\Phi_\nu(\vec{r})$ as normalized bonding and antibonding combinations of *s-p* hybridized orbitals, respectively.[30] The label $\nu=(1,2,3,4)$ stands for the four tetrahedral directions [111], $[1\bar{1}\,\bar{1}]$, $[\bar{1}1\bar{1}]$, and $[\bar{1}\,\bar{1}1]$ in the order. By an extension of standard arguments used to reduce the number of independent matrix elements of a local Hamiltonian between pairs of local orbitals centered at different lattice sites,[46] the number of the parameters $\langle \Phi_\nu(\vec{r}) \mid \Sigma(\vec{r},\vec{r}';E) \mid \Phi_{\nu'}(\vec{r}'-\vec{l}) \rangle$ can be considerably reduced by utilizing the symmetry properties (2.13) and (2.14) and the assumed reality of the local orbitals. Specifically, the minimal set of ten independent matrix elements listed in Table I is obtained by extending the lattice vector $\vec{l}$ up to second nearest neighbor unit cells.

The Hartree-Fock band eigenvalues of diamond to be used as input to our fitting were taken from the recent self-consistent calculation by Mauger and Lannoo.[47] The parameters $\epsilon_0-\epsilon_6$ (cf. Table I) were at first obtained from the knowledge of the energy eigenvalues at the high-symmetry points Γ, X, and L. The parameters ϵ_7, ϵ_8, and ϵ_9 were then determined by fitting the shape of the bands along the symmetry lines Δ and Λ connecting these points; at the same time, the parameters ϵ_1, ϵ_3, and ϵ_5 were readjusted for each trial set of values of the shape-fitting parameters $\epsilon_7-\epsilon_9$ so as to leave unchanged the energy eigenvalues at the high-symmetry points. Actually, we expect this procedure to limit the degree of arbitrariness of the parameters that is inherent to any Slater-Koster fit.

TABLE I. "Best estimate" values of the parametric integrals for the Hartree-Fock and the $X\alpha$ band structures of diamond.

Parameter name	ν	ν'	$\vec{l}$[a]	HF valence[b] (eV)	HF conduction[b] (eV)	$X\alpha$ valence[c] (eV)	$X\alpha$ conduction[c] (eV)
ϵ_0	1	1	0	−15.3687	18.2813	−9.8844	9.1719
ϵ_1	1	2	0	−2.6646	−0.6296	−1.4844	−0.0490
ϵ_2	1	1	$\frac{a}{2}(1,1,0)$	1.2198	−1.1302	0.8203	−0.6724
ϵ_3	1	2	$\frac{a}{2}(1,1,0)$	−0.4463	1.5438	−0.5844	0.5479
ϵ_4	1	1	$\frac{a}{2}(1,\bar{1},0)$	−0.5011	0.4740	−0.3172	0.2318
ϵ_5	1	2	$\frac{a}{2}(0,1,\bar{1})$	−0.1640	−0.2315	−0.0622	−0.1172
ϵ_6	1	1	$\frac{a}{2}(2,0,0)$	−0.0323	−0.0990	0.0318	−0.0339
ϵ_7	1	2	$\frac{a}{2}(1,\bar{1},0)$	0.02	−0.10	0.175	0.1495
ϵ_8	1	2	$\frac{a}{2}(0,\bar{1},\bar{1})$	0.10	0.14	−0.400	−0.300
ϵ_9	1	2	$\frac{a}{2}(2,0,0)$	0.04	−0.18	−0.055	−0.989

[a]The meaning of the indices ν, ν', and $\vec{l}$ is specified in the text. a is the lattice constant (6.7269 a.u.).
[b]Fitted from the Hartree-Fock band structure of Ref. 47.
[c]Fitted from the $X\alpha$ band structure of Ref. 7.

The "best values" of the ten Hartree-Fock parameters for both sets of valence and conduction bands of diamond are listed in Table I.

We remark that the value of the parameter ϵ_0 (where the orbitals are located at the same lattice site and point along the same tetrahedral bond) corresponds to the *absolute* energy scale which is provided by the Hartree-Fock calculation. In particular, the top of the valence bands at Γ is set at −4.0 eV by the calculation of Mauger and Lannoo.[47] This is an additional information that can be extracted from a Hartree-Fock but not from an ordinary band calculation where the zero of the energy scale is set arbitrarily.

B. The one-particle Green's function

We pass now to the calculation of the matrix elements (2.33). To this end, we can considerably reduce the amount of numerical labor by making the approximation of retaining in the expression (2.34) of the matrix $W'(\vec{q};E)$ only the terms with $\vec{m}=\vec{m}'=0$ and with the bonds σ parallel to τ and σ' parallel to τ'. On the other hand, the indices of summation on the right side of Eq. (2.34) extend over a wider range needed to a better convergence that will be specified in the next subsection. With this approximation the matrix elements (2.33) become

$$\langle \Phi_{b_i}(\vec{r}) \mid \Sigma'(\vec{r},\vec{r}';E) \mid \Phi_{a_j}(\vec{r}'-\vec{t}) \rangle$$

$$= \frac{i}{2\pi} \int_0^\infty dE' [\bar{G}^{(v)}_{b_i b_j}(-\vec{t};E,E') W'_{b_i b_i b_j b_j}(\vec{t};E') + \bar{G}^{(c)}_{a_i a_j}(-\vec{t};E,E') W'_{a_i b_i a_j b_j}(\vec{t};E')] \quad (3.1)$$

for the valence bands [the subscript b stands for bonding orbitals and $(i,j)=(1,2,3,4)$], and

$$\langle \Phi_{a_i}(\vec{r}) \mid \Sigma'(\vec{r},\vec{r}';E) \mid \Phi_{a_j}(\vec{r}'-\vec{t}) \rangle$$

$$= \frac{i}{2\pi} \int_0^\infty dE' [\bar{G}^{(v)}_{b_i b_j}(-\vec{t};E,E') W'_{b_i a_i b_j a_j}(\vec{t};E') + \bar{G}^{(c)}_{a_i a_j}(-\vec{t};E,E') W'_{a_i a_i a_j a_j}(\vec{t};E')] \quad (3.2)$$

for the conduction bands (the subscript a stands for antibonding orbitals). We have introduced the notation

$$W'_{\sigma_i\tau_i\sigma_j\tau_j}(\vec{t};E)=\frac{1}{\mathcal{N}}\sum_{\vec{q}}^{BZ} e^{-i\vec{q}\cdot\vec{t}}\, W'_{0\sigma_i\tau_i,0\sigma_j\tau_j}(\vec{q};E)\ . \tag{3.3}$$

Note that in Eqs. (3.1) and (3.2) the summation over bands in the definition (2.22) of the matrix elements of the Green's function has been explictly separated into occupied (v) and unoccupied (c) bands. In particular, in our calculation we shall include only the four valence and the four conduction bands, thereby neglecting the contribution of high excited bands for which the energy denominators get larger and the effective overlap between the wave functions get smaller. Owing to the reality of the local orbitals, we may split the real and imaginary parts of $G^{(v)}$ and $G^{(c)}$ as follows:

$$G^{(v)}_{b_ib_j}(-\vec{t};E)=\mathcal{P}\int_{-\infty}^{+\infty} dE'\frac{\gamma^{(v)}_{b_ib_j}(-\vec{t};E')}{E-E'} + i\pi\gamma^{(v)}_{b_ib_j}(-\vec{t};E) \tag{3.4}$$

and

$$G^{(c)}_{a_ia_j}(-\vec{t};E)=\mathcal{P}\int_{-\infty}^{+\infty} dE'\frac{\gamma^{(c)}_{a_ia_j}(-\vec{t};E')}{E-E'} - i\pi\gamma^{(c)}_{a_ia_j}(-\vec{t};E)\ , \tag{3.5}$$

where the symbol $\mathcal{P}$ means that the principal value of the integrals has to be taken and where the real functions $\gamma^{(v)}_{b_ib_j}(-\vec{t};E)$ and $\gamma^{(c)}_{a_ia_j}(-\vec{t};E)$ are defined as

$$\gamma^{(v)}_{b_ib_j}(-\vec{t};E)=\sum_{\{v\}}\frac{1}{\mathcal{N}}\sum_{\vec{k}}^{BZ} e^{-i\vec{k}\cdot\vec{t}}\, c_{b_iv}(\vec{k})c^*_{b_jv}(\vec{k}) \times\delta(E-E_v(\vec{k}))\ , \tag{3.6}$$

$$\gamma^{(c)}_{a_ia_j}(-\vec{t};E)=\sum_{\{c\}}\frac{1}{\mathcal{N}}\sum_{\vec{k}}^{BZ} e^{-i\vec{k}\cdot\vec{t}}\, c_{a_ic}(\vec{k})c^*_{a_jc}(\vec{k}) \times\delta(E-E_c(\vec{k}))\ . \tag{3.7}$$

Expressions (3.6) and (3.7) can be calculated by standard methods of integration over the Brillouin zone once the band structure is known. As we have already discussed while commenting on Eq. (2.20), the band structure to be used in Eqs. (3.6) and (3.7) should be as close as possible to what is expected to be the outcome of our calculation. For this reason we have taken it from a previous $X\alpha$ calculation[7] that already includes exchange and correlations even though in an approximate way. The "best values" of the Slater-Koster fitting parameters for this $X\alpha$ band structure have been given in Ref. 30 but are also reported in our Table I for a prompt identification of the indices $(\nu,\nu',\vec{1})$. We note that the value of the parameter ϵ_0 corresponds to setting the top of the correlated valence bands at -1.5 eV on the absolute energy scale. This implies an initial guess of 2.5 eV for the upward shifting of the top of the valence bands with respect to the Hartree-Fock value. However, our calculation will actually set the top of the valence bands at 0.25 eV so that a suitable adjustment of the energy scale for the Green's function will be required.

The functions (3.6) and (3.7) whose indices $(i,j,\vec{t})$ run over the set of Table I, have been calculated performing the summation over $\vec{k}$ by the linear tetrahedron method.[48] Having partitioned the irreducible wedge of the Brillouin zone into 754 tetrahedra, for each band the density of states contributed by a selected tetrahedron was multiplied by the value of the integrand in Eqs. (3.6) and (3.7), taken first at the "center of mass" $\vec{k}_c$ of the selected tetrahedron, and then summed over the corresponding values at the star of $\vec{k}_c$. Once the functions (3.6) and (3.7) have been calculated over the entire energy range spanned by the valence and conduction bands, respectively, with a step of 0.25 eV, the real part of $G^{(v)}$ and $G^{(c)}$ were obtained by evaluating the principal-value integrals in Eqs. (3.4) and (3.5) where the singularities at $E=E'$ were isolated using standard procedures.[49]

C. The screened interaction

There remains to calculate the three types of matrix elements (3.3) entering Eqs. (3.1) and (3.2). The linear tetrahedron method, which we have used to calculate the Green's functions, cannot be adopted to perform the $\vec{q}$ integration in Eq. (3.3) because it is quite costly to generate the matrix $W'(\vec{q};E)$ over a fine mesh of points in the Brillouin zone as required by that method. The special points method,[50] on the other hand, cannot be applied either because the matrix elements

$W'_{0\sigma_i\tau_i,0\sigma_j\tau_j}(\vec{q};E)$ are not smooth functions of $\vec{q}$ when $\sigma=\tau=b$ or $\sigma=\tau=a$, behaving like $|\vec{q}|^{-2}$ about $\vec{q}=0$. This behavior can be checked by recalling the limit of $\chi(\vec{q},\vec{q};E)$ as $\vec{q}\to 0$.[51] To integrate over the Brillouin zone functions with these types of singularities and yet keep the number of mesh points rather limited, the special directions method by Bansil[52] seems thus to provide the most suitable procedure. According to this method, when a function has a weak angular dependence around the center of the Brillouin zone even though it might be singular there, to a good degree of approximation one can evaluate its integral over the Brillouin zone by calculating only one-dimensional integrals over an optimally chosen set of directions determined by the condition that suitable linear combinations of cubic harmonics (up to a given order) vanish on that set. In our calculation we have taken the minimal set which consists simply of the line

$$(k_x,k_y,k_z)=\frac{2\pi}{a}(0.83539,0.40747,0.25714)\zeta \quad (0\le\zeta\le 1) \tag{3.8}$$

in the irreducible wedge of the Brillouin zone, and of all the other lines related to this one by cubic symmetry. This minimal set takes explicitly into account the angular variation carried by the totally symmetric cubic harmonics up to $l=6$. We have then selected eleven equally spaced points along the line (3.8), including the extrema at the center ($\zeta=0$) and on the boundary ($\zeta=1$) of the Brillouin zone.

In spite of the considerable reduction in the number of $\vec{q}$ points where the matrix elements $W'_{0\sigma_i\tau_i,0\sigma_j\tau_j}(\vec{q};E)$ need to be generated by using the special directions method, the sum over the star of any given mesh point along the special line (3.8) was still prohibitively time-consuming. We were thus urged to fully exploit the transformation properties of the matrix elements $W'_{0\sigma_i\tau_i,0\sigma_j\tau_j}(\vec{q};E)$ as $\vec{q}$ is replaced by $R\vec{q}$, R being an operation belonging to the cubic group O_h. These properties, which are altogether nontrivial as they involve complex $\vec{q}$ dependent phase factors, can be obtained from the knowledge of the symmetry properties of the polarization matrix $\chi(\vec{q}+\vec{G},\vec{q}+\vec{G}';E)$ and of the transformation law of the local orbitals under the operations of the crystal space-group. The effort is, however, largely rewarded by the gain in computing time which is reduced by about a factor of 10.

The local orbitals $\Phi_\nu(\vec{r})$ we used in our calculation were expressed as linear combinations of Gaussian functions; the coefficients of the expansion and the exponents of the Gaussians were determined in Ref. 30 by optimizing the overall agreement between the dipole and current forms of the optical response within the RPA approximation without local-field effects. The justification for this criterion is also a pragmatic one in that two-particle excitations are found in quantitative agreement with a variety of experimental facts.[30] We remark that pairs of these orbitals pointing along different bonds or centered at different lattice sites are not exactly orthogonal as they should be in principle, the larger overlap integrals being of the order of 0.1. We have remedied this shortcoming when strictly necessary (as, for instance, to avoid divergencies) by forcing the overlap integrals to be identically zero, but we have not bothered about the not-exact orthogonality otherwise. In particular, the overlap matrix which should be present on the right-hand side of the eigenvalue equation (2.16) has been set equal to the identity matrix.

We found it sufficient to extend the lattice vectors $\vec{l}$ in the generalized form factors (2.26) up to the first-nearest neighbors while the pair of indices ν and μ refers either to the same bond or to adjacent bonds. In addition, the indices (ν,ν') and (μ,μ') that label the screening matrix $S(\vec{q};E)$ in Eq. (2.25) were further restricted to represent bonding and antibonding orbitals, respectively, thereby reducing the dimensionality of that matrix to 28×28. However, one may verify that this limited labeling is exact only within the RPA approximation whereas it holds approximately within the TDSHF approximation since the exchange matrix (2.30) does not bear the same symmetry properties as the Coulomb matrix (2.29) under the interchange of ν with μ.

The Coulomb matrix (2.29) was calculated at the chosen $\vec{q}$ points along the special line (3.8) from its definition in terms of the rapidly convergent sum over the reciprocal lattice vectors $\vec{G}$ rather than of its slowly convergent Fourier expression.[53] The exchange matrix (2.30), on the other hand, can be calculated from its definition in terms of a Fourier transform by retaining only the term with $\vec{m}=0$ owing to the localization of the local orbitals. The resulting expression is then $\vec{q}$ independent. Moreover, we found it very important to take proper

care of the screened potential $v_s(\vec{r}-\vec{r}')$ in the exchange matrix. We have approximated $v_s(\vec{r}-\vec{r}')$ by the phenomenological form given by Srinivasan[54] that we have found, on the whole, to be a reasonable spherical approximation to the full linear response screening of a point impurity in diamond.[55]

The RPA irreducible polarizability $N(\vec{q};E)$ was calculated in Ref. 30 over the whole optical range but at $\vec{q}=0$ only. Extending that calculation now at the chosen $\vec{q}$ points along the special line requires a considerable effort which we have thought possible to avoid by arguing that the $\vec{q}$ dependence of the matrix $N(\vec{q};E)$ may be regarded as being rather weak. To substantiate this argument, we have calculated the RPA static dielectric function without local-field effects along the special line (3.8) from the expression

$$\epsilon(\vec{q};E=0)=1-\frac{v(\vec{q})}{\Omega_0}\sum_{\vec{\Gamma}\nu\mu}\sum_{\vec{\Gamma}'\nu'\mu'}A_{\vec{\Gamma}\nu\mu}(\vec{q})N_{\vec{\Gamma}\nu\mu,\,\vec{\Gamma}'\nu'\mu'}(\vec{q}=0;E=0)A^{*}_{\vec{\Gamma}'\nu'\mu'}(\vec{q})\,, \tag{3.9}$$

that is, by taking the matrix $N(\vec{q};E=0)$ at $\vec{q}=0$ and letting the $\vec{q}$ dependence be carried only by the generalized form factors. To reduce the effect of anisotropy, Eq. (3.9) was then averaged over the star of the special line and the result was compared with Penn's interpolation formula[28] properly normalized to the value 4.8 of the expression (3.9) at $\vec{q}=0$. The rather good agreement between the two functions, as shown in Fig. 2, is a strong indication that the $\vec{q}$ dependence of the N matrix may indeed be neglected without making too serious errors. This approximation might get worse at nonzero values of the frequency, expecially when one is after $\vec{q}$ dependent features. Nevertheless, we regard it as sufficient for our ultimate purpose of calculating the matrix elements (2.33) since they involve additional averaging over the Brillouin zone.

We discuss now the energy-dependence of the matrix elements (3.3) of the screened interaction. We first note that the overall shape of different matrix elements is expected to be quite similar since it is controlled by the screening matrix $S(\vec{q};E)$ which is common to all of them. The upper limit of the energy integration in Eqs. (3.1) and (3.2) is thus determined by the common range of these matrix elements and has to be set far enough to exhaust the main features of the inverse dielectric matrix, namely, the electron-hole continuum and the plasma resonance. The experimental value of the plasma resonance in diamond is at about 33.3 eV.[56] This value has to be compared with the electron gas value of 31.3 eV obtained with an average electronic density of eight electrons per unit cell, the upward shift being attributed to the interaction of the plasma resonance with the electron-hole continuum at its lower energy side.[57] The theoretical position of the plasma resonance at $\vec{q}=0$ could be obtained by first calculating the optical constants $\epsilon_1(E)$ and $\epsilon_2(E)$ from Eq. (2.25) with $\vec{G}=\vec{G}'=0$ in the $\vec{q}\to 0$ limit, and by then locating the zero of $\epsilon_1(E)$ in the region where $\epsilon_2(E)$ is small. However, the $X\alpha$ band structure that we have taken as input to our calculation yields a joint density of states for the valence to conduction bands transitions that terminates already at 34 eV, thereby shifting further the zero of $\epsilon_1(E)$ to about 38 eV and leading to a delta function profile for the plasma resonance. This shortcoming originates from the overshrinking of both the gap and the valence bandwidth which is common to the local approximations of exchange and correlations,[6,7] as we shall discuss in the next section. These circumstances, however, are favorable to extract the contribution of the electron-hole continuum to the sum rule for $-\mathrm{Im}[\epsilon^{-1}(E)]$ which[26] was found to be of about 10%. (In metals, on the other hand, the plasmon pole alone exhausts the sum rule for small $\vec{q}$.) In fact, by summing numerically over the electron-hole continuum and including properly the strength of the plasmon

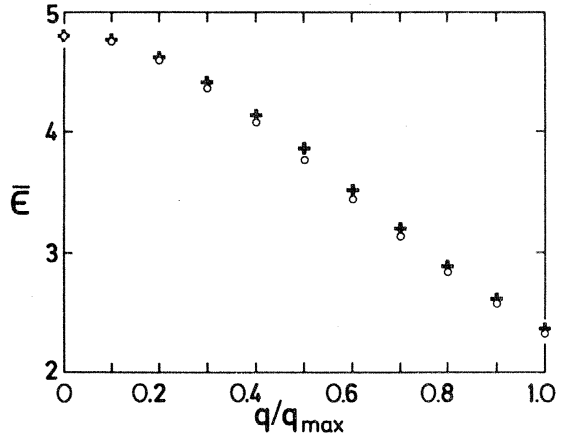

FIG. 2. Comparison of the RPA $\epsilon(\vec{q};E=0)$ (averaged over the star of $\vec{q}$ along the special line) calculated with a $\vec{q}$-independent N matrix (+) with the (spherical) Penn's interpolation formula (○).

delta function, the sum rule for $-\mathrm{Im}[\epsilon^{-1}(E)]$ came out correctly to have the same value, to within 1%, of the sum rule for $\epsilon_2(E)$.

To include the delta function numerically without modifying the bulk of our input data, we have simply extended the last nonzero values of the matrix elements $N(\vec{q};E)$ up to a maximum energy of 40.5 eV, value which has proven sufficient for the calculation of the energy bands of diamond. Owing to the resulting numerical inaccuracy, the sum rule for $-\mathrm{Im}[\epsilon^{-1}(\vec{q},\vec{q};E)]$ calculated at the eleven mesh points along the special line lagged behind the corresponding sum rule for $\epsilon_2(\vec{q},\vec{q};E)$ on the average by about 10%. Besides, the latter sum rule did not maintain the expected constant theoretical value at different $\vec{q}$ but it was found to be monotonically decreasing for increasing $|\vec{q}|$, reducing at the boundary of the Brillouin zone to about half its value at the center. This fact is an indication that transitions to higher conduction bands should be included in order to fulfill the Thomas-Reich-Kuhn sum rule at finite $\vec{q}$. In practice, however, this inclusion is not essential for the calculation of the matrix elements (3.1) and (3.2) because the weight function there behaves like E'^{-1} for large E' in contrast to the weight function in the sum rule which is E'. In the next section we shall make an estimate of how the improper inclusion of the plasma resonance could influence the lower portion of the valence bands.

In Figs. 3 and 4 we have reported as functions of the energy the main matrix elements (3.3) for

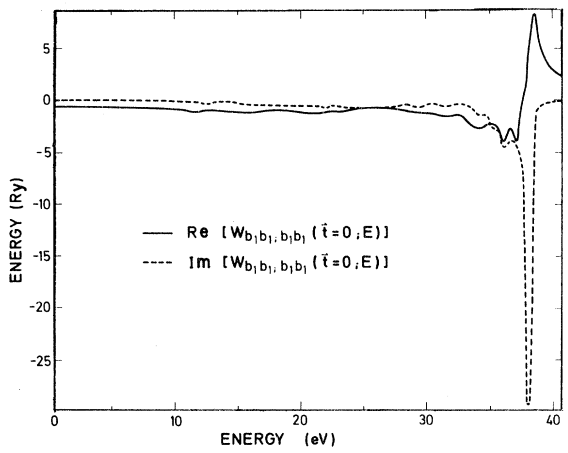

FIG. 3. Energy dependence of the main matrix element of the induced part of the dynamically screened potential between two pairs of bonding orbitals centered at the same site and pointing along the same bond [1,1,1].

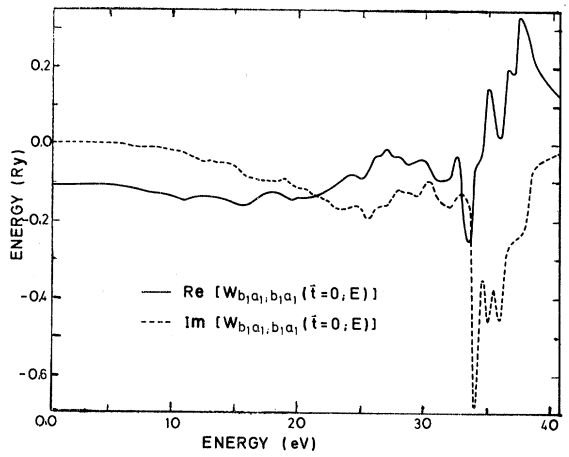

FIG. 4. As in Fig. 3 for two pairs of bonding-antibonding orbitals.

the two cases *bb-bb* and *ba-ba* entering Eq. (3.1) in the order. Note that the first is about an order of magnitude larger than the second owing to the fact that, as $|\vec{q}+\vec{G}|\to 0$, the generalized form factors (2.26) have a finite limit in the first case but not in the second. This remark implies, in particular, that the approximation of retaining only the $\vec{m}=0$ term in the calculation of the matrix elements (2.29) of the Coulomb potential, as it has been done to obtain the inverse dielectric function directly in real space,[58] would lead to self-energy corrections that are too small and even of the wrong sign.

As we have previously discussed, the energy dependence of other matrix elements (3.3) is quite similar to those reported in Figs. 3 and 4. On the contrary, the matrix elements $G_{\sigma_i\sigma_j}(\vec{t};E)$ of the Green's function show a rather different energy dependence for different values of the indices $(i,j,\vec{t})$ because of the presence of the energy delta function in their definition [cf. Eqs. (3.6) and (3.7)]. Specifically, these matrix elements show an oscillatory behavior as function of the energy which is more pronounced for increasing $|\vec{t}|$. In fact, it is precisely this oscillatory behavior, together with the fact that the matrix elements of the screened potential are rather energy independent over most of their range (barring the region about the plasma resonance) which leads to the short-range property of the self-energy operator once the convolution integrals in Eqs. (3.1) and (3.2) are performed. (We have used Simpson's rule with a step of integration of 0.25 eV.) We have indeed verified numerically that, on the average, over the whole

energy spectrum, the matrix elements (3.1) and (3.2) get progressively smaller (even by several orders of magnitude) as $|\vec{t}|$ gets larger.

Once the matrix elements (2.17) and (2.18) have thus been calculated, the self-consistent non-Hermitian eigenvalue problem (2.16) was solved by performing the diagonalization (better, the block diagonalization in general) at a fine mesh of energy values (with a step of 0.25 eV) and by looking then at the local minima of the functions $|E-E_n(\vec{k})|$ for given wave vector $\vec{k}$ and band index n. The numerical subroutine which we have used to calculate the eigenvalues of a general (non-Hermitian) matrix was tested to work properly in cases where degeneracies occur because problems related to the fact that the matrix is not semisimple might show up there.[59] The resultant band structure is presented in the next section.

IV. RESULTS AND DISCUSSION

The quasiparticle valence and conduction band structure of diamond [that is, the *real* part of the eigenvalues $E_n(\vec{k})$ of Eq. (2.16)] is displayed in Fig. 5 for two symmetry directions. The label EXC signifies that the full screening matrix (2.27) including both local-field effects and the electron-hole attraction has been used to calculate the wave vector and energy-dependent dielectric matrix. The Hartree-Fock (HF) band structure by Mauger and Lannoo is also shown for comparison. The energy eigenvalues at the high-symmetry points Γ, X, and L for the HF and EXC calculations are reported in columns 1 and 2 of Table II, respectively. We note the following features.

(i) Self-energy corrections make the valence bands moving upwards and the conduction bands moving downwards on the absolute energy scale, thereby reducing the amount of energy required to produce an electron-hole pair. This result matches the general trends of correlation corrections as obtained, e.g., by the configuration interaction formalism.[14] Note, in particular, that the drastic reduction of the band gap at Γ from the Hartree-Fock value (15.0 eV) to the final correlated value (7.4 eV) results from a combined positive shift of

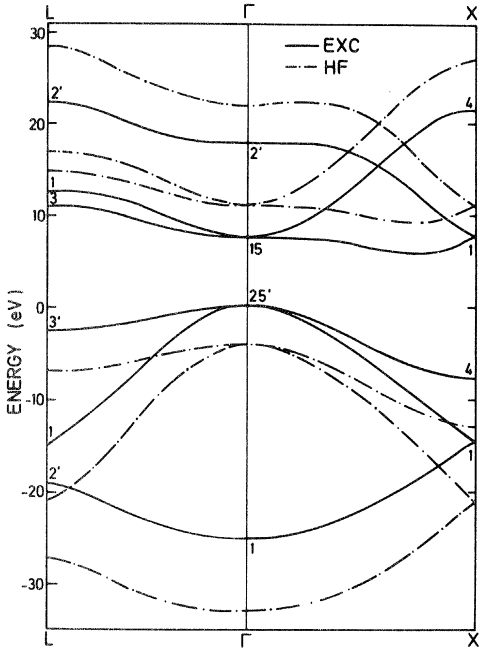

FIG. 5. Comparison of the quasiparticle band structures of diamond calculated within the Hartree-Fock approximation (from Ref. 47) (dashed-dotted line) and within the GW approximation with the screening taken within the TDSHF approximation (full line).

TABLE II. Band structure of diamond at the high-symmetry points Γ, X, and L for the HF, EXC, and RPA calculations. Values are given in eV relative to the respective top of the valence bands. v and c denote valence and conduction, respectively.

	HF	EXC	RPA		HF	EXC	RPA
Γ_1^v	−29.0	−25.2	−26.1	X_4^c	31.0	21.35	22.8
$\Gamma_{25'}^v$	0.	0.	0.	$L_{2'}^v$	−23.1[a]	−19.7	−20.75
Γ_{15}^c	15.0	7.4	8.25	L_1^v	−17.0	−15.0	−15.5
$\Gamma_{2'}^c$	26.0	17.6	18.9	$L_{3'}^v$	−3.1	−2.8	−2.9
X_1^v	−17.0	−14.75	−15.25	L_3^c	19.0	11.0	11.85
X_4^v	−9.0	−7.9	−8.2	L_1^c	21.0	12.6	13.75
X_1^c	15.0	7.45	8.3	$L_{2'}^c$	32.5[a]	23.3	24.5

[a]There exists some uncertainty about this value.

the top of the valence bands by 4.25 eV and a negative shift of the bottom of the conduction bands by 3.35 eV, a result which is in agreement with the general "rule of thumb" that "to larger effective masses correspond larger self-energy corrections."[14,15] Our value for the optical band gap is in very good agreement with the experimental value of 7.3 eV obtained by reflectivity experiments.[8]

(ii) At any given $\vec{k}$ vector, the magnitude of the self-energy corrections increases away from the gap region. For the valence bands the net result is then a narrowing of the bandwidth, which again is in agreement with general trends.[14] In particular, the Hartree-Fock bandwidth (29.0 eV) is reduced to 25.2 eV by our calculation, a value which is rather close to the experimental value of 24.2 ± 1 eV obtained by x-ray photoemission.[9] On the other hand, the value given by Brener in his calculation using the (energy-independent) COHSEX approximation is 27.2 eV.[23] We will discuss below the reasons why we indeed expect an energy-independent approximation for the self-energy to fail away from the gap. Here we comment that we have made a pessimistic estimate of how the approximate numerical inclusion of the plasma resonance, as discussed in Sec. III C might influence the width of the valence bands, the result being that it could at most be reduced to a value of 23.6 eV.

(iii) The self-energy corrections show a noticeable $\vec{k}$ dependence, being in general more pronounced away from the center of the Brillouin zone. The indirect absorption edge is found about at $\vec{k}_c=(0.75,0,0)2\pi/a$ with magnitude 5.70 eV, in close agreement with the experimental values.[60]

Figure 6 compares the quasiparticle band structure EXC obtained by using the full screening matrix (2.27) that includes the electron-hole attraction, with its RPA simplified form obtained by setting $V^x=0$ in Eq. (2.27). The magnitude of the self-energy corrections in the RPA approximation are manifestly smaller than the corresponding values in the TDSHF approximation; in particular, the RPA bandwidth and gap are increased by about 1 eV compared to the full calculation. (See also column 3 of Table II.) This result indicates that there exists a need to be as accurate as possible in the calculation of the two-particle Green's function (the inverse dielectric matrix being obtained from a degenerate form of it) to get a satisfactory description of the single-particle spectrum. In addition, this result provides an *a posteriori* answer to the

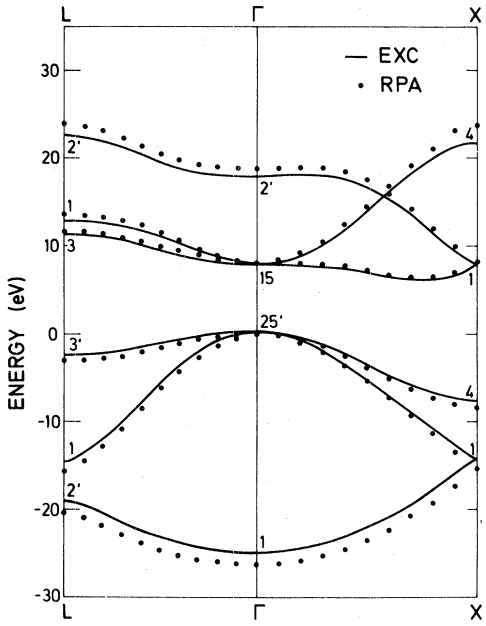

FIG. 6. Comparison of the quasiparticle band structures of diamond calculated within the GW approximation with the screening taken within the TDSHF approximation (full line) and within the RPA approximation (dotted line).

question of the internal consistency of the theory that we have left open in Sec. II A.

It is important to emphasize at this point that our RPA and TDSHF dielectric matrices do *not* contain any adjustable parameter to be fitted to experimental data such as the long wavelength static dielectric constant ϵ_0. The *ab initio* values we get for ϵ_0 are 4.25 and 6.10, respectively, thereby fulfilling the other "rule of thumb" which has emerged from model calculations[15] that "self-energy corrections increase with ϵ_0." However, we think that a warning should be made against the temptation of utilizing an RPA functional form of the dielectric matrix with an empirically adjusted ϵ_0 (as in the Penn's model) on the basis of the following considerations. Since the self-energy operator is a short-range kernel, the dielectric matrix needs to be correctly described for relatively large values of $\vec{q}$ and $\vec{G}$ where it is known that exchange and correlations become most important.[61] In fact, this was precisely the context where in the literature[15] was already felt the need of using dielectric functions improved over the RPA approximation to describe properly the exchange-correlation hole about each electron.

Note from Figs. 5 and 6 that, on the absolute energy scale, the top of the valence bands is shifted

from the Hartree-Fock value of -4.0 eV to 0.25 eV in the full EXC calculation and to -0.15 eV in the RPA calculation. These values correspond to the position of an ideal vacuum level whose position is not affected by the presence of a physical surface. Therefore, if one could calculate with sufficient accuracy the shift of the bulk vacuum level caused by the presence of a physical surface, such as the surface dipole barrier, then it would be also possible to state, for instance, whether or not the material has a negative electron affinity. Since typical estimates of surface dipole potential in metals range about from 2 eV up to 5 eV,[62] one would be tempted to conclude that diamond has a negative electron affinity with its vacuum level lying within the fundamental gap below the conduction-band minimum, even though this kind of behavior would be rather unusual for a pure covalent solid. Unfortunately, it is not easy to extend these estimates to nonmetals, and thus no convincing theoretical claim can be advanced. However, in spite of our circumspection, a recent photoemission experiment[63] has clearly shown that indeed diamond has a negative electron affinity with a large quantum efficiency.

We focus now on the question raised in the Introduction about the relative weight of the coupling to the propagation of a quasiparticle of the two different kinds of elementary excitations contributing to the dynamical screening of a scalar longitudinal perturbation in the crystal (namely, electron-hole pairs and plasmons). To this end, we have performed an additional calculation where the plasmon contribution to the self-energy is cut off by restricting the energy integration in Eq. (2.33) up to 32.0 eV only, that is, before the onset of the plasma resonance. The results are that (to within our numerical error that we have estimated to be about ± 0.2 eV) the optical gap is found to be practically unchanged whereas the valence bandwidth has increased to 26.45 eV (cf. the entries labeled EH in Table III). We may thus argue that the properties of the quasiparticles in the vicinity of the top of the valence and the bottom of the conduction bands are basically determined by the coupling to the electron-hole excitations, whereas predominantly nonlocal plasmon-type correlations introduce a shrinking of about 1.25 eV in the valence bandwidth. Since the electron-hole correlation effects are predominantly of short-range character, we might conclude that correlation in the vicinity of the band gap can be accounted for by a "local" description (that is, depending only on the local environment and thereby not properly including long-range correlation effects such as plasmons) along the lines of the work of Sham and Kohn and others.[11,12,64] Recent work on metallic surfaces[27] has indeed shown that a local density approximation correctly describes the large $\vec{q}$ portion of a wave-vector decomposition of the total ground-state exchange-correlation energy of an electron gas whereas it fails badly at small $\vec{q}$, but this failure in the end is rather unimportant because of phase space considerations. Our argument, however, does *not* necessarily imply that the local density approximation (LDA) in its formulation for the ground state[3,4] can correctly describe low-lying excited states of the crystal. In fact, previous LDA calculations, which in addition made use of a local exchange-correlation operator, have given values for the direct band gap in diamond of 6.3 eV (Ref. 6) and 5.8 eV (Ref. 7) which are too small compared with the experimental value (7.3 eV). The same situation occurs for Si where a LDA calculation gives a direct gap of 2.5 eV (Ref. 10) versus the experimental 3.4 eV. We believe, however, that such an underestimate of the values of the band gaps occuring in the LDA approximation is mainly due to the use of a local (and energy-independent) exchange-correlation operator which overestimates the effects of screening over and above the Hartree-Fock approximation, rather than to the inadequacy of a "local" description of the nonlocal self-energy operator itself. The fact that approximations using local operators produce band gaps that are systematically smaller than experiment appears indeed to be a general trend.[18,65] A similar situation occurs also for the bandwidths. For diamond, in particular, LDA calculations using local exchange-correlation operators have given

TABLE III. Comparison of the experimental band gap and valence bandwidth of diamond with values from different calculations (in eV).

	Expt.	HF[c]	EXC[d]	RPA[d]	EH[d]	COHSEX[d]	LDA[e]
E_{gap}	7.3[a]	15.0	7.4	8.25	7.4	7.2	6.3
ΔE_{val}	24.2 ± 1[b]	29.0	25.2	26.1	26.45	28.85	20.4

[b]From Ref. 9.
[c]From Ref. 47.
[d]This work.
[e]From Ref. 6.

values for the valence bandwidth of 20.4 eV (Ref. 6) and 20.6 eV (Ref. 7) compared to the experimental (XPS) value 24.2 ± 1 eV,[9] but again this appears to be a general trend.[65,10] As a matter of fact, the need of using a nonlocal exchange-correlation potential has repeatedly been invoked in the past.[66]

The need for an energy-dependent potential has also been realized.[67] The same need results from our calculation, too. In fact, as it can be seen from Figs. 3 and 4, chopping out the plasmon-pole contribution is in effect equivalent to approximating the screened interaction (and, therefore, the self-energy itself) by an almost energy-independent quantity. To get closer to a truly energy-independent approximation for the self-energy, we have mimicked the often used COHSEX approximation[2,20] by taking the value of the matrix elements (3.3) at $E=0$ and then extending it throughout the chosen range of integration (i.e., up to 40.5 eV). (Notice, however, that in this way we do *not* evaluate the self-energy corrections *exactly* within the COHSEX approximation which derives from an analytical rather than a numerical approximation.) The energy-gap is found in rather good agreement (7.2 eV) with our previous results whereas the valence bandwidth now comes out to be essentially unrenormalized (28.85 eV) with respect to the Hartree-Fock value (cf. Table III). This result suggests that an energy-independent approximation works well at energies about the gap, as it is implied in the derivation of the COHSEX approximation itself[2] and as it has already been remarked explicitly.[68] As soon as we leave the gap region moving down through the valence bands, however, the energy-dependence of the self-energy becomes progressively important, corresponding to the increasing weight of the plasma resonance. We have shown this effect to be conspicuous for a material, such as diamond, with a wide valence bandwidth, but we expect the argument to hold more generally for other wide-band materials, such as Si. Our conclusion matches the finding of a nonlocal energy-dependent pseudopotential calculation for Si.[69]

Finally, we comment on the decay of quasiholes in diamond. Figures 7 and 8 show the imaginary versus the real part of the quasiparticle levels $E_n(\vec{k})$ with a hole in the valence bands along two symmetry directions and within the EXC and RPA approximations, respectively. The corresponding lifetime of these approximate $(N-1)$ particle excited states is given by $\{2\,\mathrm{Im}[E_n(\vec{k})]\}^{-1}$. Since the mechanism responsible for the decay of the quasiholes is the Coulomb interaction among the particles, we can call the radiationless transition to a final state with more than one hole in the valence bands an intraband Auger process that can be single, double, etc. We notice from Figs. 7 and 8 that the decay rate vanishes (to within our numerical error) below a threshold. In fact, from the elementary treatment of the Auger transitions we would expect this threshold to be at $E^v_{\Gamma_{25'}}-E_{\mathrm{gap}}=-7.15$ eV. However, since the first and most prominent broad peak of the valence density of states has its half-maximum at about -1.5 eV, the decay rate is expected to become noticeable starting from about -10.5 eV. This expectation is indeed confirmed by our (EXC) calculation which also shows a rather sharp rise beyond the threshold. Direct comparison of our results with the experimental data (obtained, e.g., by photoemission experiments) does not seem possible mainly because of uncertainties in extracting the relevant experimental information. Nevertheless, the values we obtain for the decay rate are in accordance with empirical broaden-

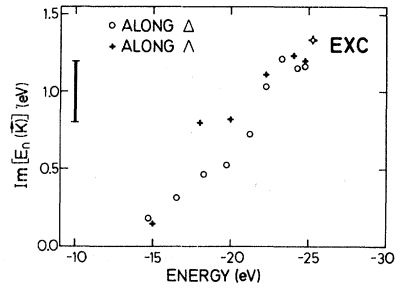

FIG. 7. Imaginary part of the quasihole levels in diamond along two different symmetry directions and within the EXC approximation (cf. Fig. 5 for the real part). The vertical bar indicates the numerical uncertainty.

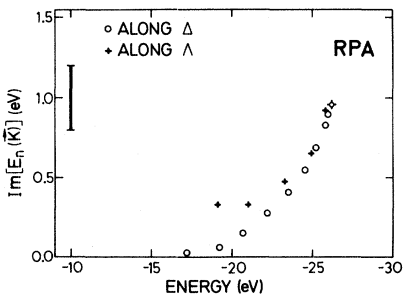

FIG. 8. As in Fig. 7 within the RPA approximation (cf. Fig. 6 for the real part).

ing factors which are necessary to relate the XPS valence-band spectra to theoretical line shapes of the electron density of states.[9,70]

V. CONCLUDING REMARKS

We have presented an investigation on the single-particle-like excitations in diamond where we have allowed the exchange-correlation potential to be nonlocal and energy-dependent. Emphasis has been placed on describing the dielectric properties of the medium as accurately as possible. The use of a local orbital basis has proven essential for this combined purpose. By studying the relative contribution of the electron-hole excitations and of the plasmon resonance to the propagation of a (quasi)particle throughout the medium, we have drawn conclusions on the validity of the local-density and of the energy-independent approximations, at least in the neighborhood of the gap (an energy region which plays a primary role in many applications). Direct extension of our method of calculation to other materials like Si appears, in principle, possible. However, here the starting point for the inclusion of dynamical correlation effects can no longer be the Hartree-Fock approximation, because of lack of Hartree-Fock calculations for heavier materials. Investigations along these lines, in particular a careful adding of correlation corrections to band eigenvalues obtained, e.g., by local-density methods, are presently under way.

ACKNOWLEDGMENTS

The authors are indebted to Professor H. Bilz, Professor P. Fulde, Professor M. Cardona, Professor R. Rosei, and especially Professor L. J. Sham and Professor W. Kohn for helpful discussions. One of us (G.S.) gratefully acknowledges receipt of a Humboldt Foundation research fellowship.

---

*Present address: Istituto di Fisica "G. Marconi," Università di Roma, 00185 Roma, Italy.

[1]See, e.g., A. L. Fetter and J. D. Walecka, *Quantum Theory of Many-Particle Systems* (McGraw-Hill, New York, 1971). In atomic calculations a many-body approach encompassing various approximations has been provided by T. N. Chang and U. Fano, Phys. Rev. A 13, 263 (1976).

[2]L. Hedin and S. Lundqvist, in *Solid State Physics,* edited by H. Ehrenreich, F. Seitz, and D. Turnbull (Academic, New York, 1969), Vol. 23, p. 1, and references therein.

[3]P. Hohenberg and W. Kohn, Phys. Rev. 136, B864 (1964); W. Kohn and L. J. Sham, *ibid.* 140, A1133 (1965).

[4]For recent developments see O. Gunnarsson and B. I. Lundqvist, Phys. Rev. B 13, 4274 (1976); O. Gunnarsson, M. Jonson, and B. I. Lundqvist, *ibid.* 20, 3136 (1979).

[5]A short summary of this work has been published in G. Strinati, H. J. Mattausch, and W. Hanke, Phys. Rev. Lett. 45, 290 (1980); W. Hanke, G. Strinati, and H. J. Mattausch, in *Recent Developments in Condensed Matter Physics,* edited by J. T. Devreese (Plenum, New York, 1981), Vol. I, p. 263.

[6]A. Zunger and A. J. Freeman, Phys. Rev. B 15, 5049 (1977).

[7]G. S. Painter, D. E. Ellis, and A. R. Lubinsky, Phys. Rev. B 4, 3610 (1971).

[8]R. A. Roberts and W. C. Walker, Phys. Rev. 161, 730 (1967).

[9]F. R. McFeely, S. P. Kowalczyk, L. Ley, R. G. Cavell, R. A. Pollak, and D. A. Shirley, Phys. Rev. B 9, 5268 (1974). However, according to recent ultraviolet photoelectron spectroscopy (UPS) data by F. J. Himpsel, J. F. van der Veen, and D. E. Eastman, Phys. Rev. B 22, 1967 (1980), the valence bandwidth in diamond should rather be 21 ± 1 eV, a value which is by about 12% smaller than the XPS value by McFeely *et al.* There are reasons to believe (L. Ley, private communication) that the UPS bandwidth might be a lower limit of the true bandwidth. Moreover, one may comment that UPS measurements could be more sensitive to the surface region than XPS measurements owing to the smaller mean free path of the escaping electron. In fact, angle-resolved XPS measurements on Cu by M. Mehta and C. S. Fadley, Phys. Rev. Lett. 39, 1569 (1977), have clearly shown that selection of the primary electrons from the surface region leads to a decreasing of the width of the *d*-band peak by about 12%.

[10]D. R. Hamann, Phys. Rev. Lett. 42, 662 (1979); L. Ley, S. Kowalczyk, R. Pollak, and D. A. Shirley, *ibid.* 29, 1088 (1972); W. D. Grobman and D. E. Eastman, *ibid.* 29, 1508 (1972).

[11]L. J. Sham and W. Kohn, Phys. Rev. 145, 561 (1966);

see also L. Hedin and B. I. Lundqvist, J. Phys. C 4, 2064 (1971).

[12]M. Rasolt and S. H. Vosko, Phys. Rev. B 10, 4195 (1974); P. A. Lee and G. Beni, *ibid.* 15, 2862 (1977).

[13]R. K. Nesbet, Adv. Chem. Phys. 9, 321 (1965).

[14]S. T. Pantelides, D. J. Mickish, and A. B. Kunz, Phys. Rev. B 10, 2602 (1974).

[15]A. W. Overhauser, Phys. Rev. B 3, 1888 (1971); J. Hermanson, *ibid.* 6, 2427 (1972); B. Lundqvist, Phys. Kondens. Mater. 6, 193 (1967).

[16]Y. Toyozawa, Prog. Theor. Phys. 12, 421 (1954).

[17]M. Inoue, C. K. Mahutte, and S. Wang, Phys. Rev. B 2, 539 (1970).

[18]A. B. Kunz, Phys. Rev. B 6, 606 (1972).

[19]D. J. Mickish, A. B. Kunz, and T. C. Collins, Phys. Rev. B 9, 4461 (1974); A. B. Kunz, D. J. Mickish, and T. C. Collins, Phys. Rev. Lett. 31, 756 (1973).

[20]L. Hedin, Phys. Rev. 139, A796 (1965).

[21]W. Brinkman and B. Goodman, Phys. Rev. 149, 597 (1966).

[22]N. O. Lipari and W. B. Fowler, Phys. Rev. B 2, 3354 (1970).

[23]N. E. Brener, Phys. Rev. B 11, 929 (1975).

[24]N. E. Brener, Phys. Rev. B 11, 1600 (1975).

[25]M. Benett and J. C. Inkson, J. Phys. C 10, 987 (1977); J. C. Inkson and M. Bennett, *ibid.* 11, 2017 (1978).

[26]D. Pines, *Elementary Excitations in Solids* (Benjamin, New York, 1964).

[27]D. C. Langreth and J. P. Perdew, Phys. Rev. B 15, 2884 (1977); W. Kohn and W. Hanke (unpublished).

[28]D. R. Penn, Phys. Rev. 128, 2093 (1962).

[29]W. Hanke and L. J. Sham, Phys. Rev. Lett. 33, 582 (1974).

[30]W. Hanke and L. J. Sham, Phys. Rev. B 12, 4501 (1975).

[31]W. Hanke and L. J. Sham, Phys. Rev. Lett. 43, 387 (1979).

[32]W. Hanke and L. J. Sham, Phys. Rev. B 21, 4656 (1980).

[33]A. J. Layzer, Phys. Rev. 129, 897 (1963).

[34]V. M. Galitskii and A. B. Migdal, Z. Eksp. Teor. Fiz. 34, 139 (1958) [Sov. Phys.—JETP 7, 96 (1968)].

[35]D. J. Thouless, *The Quantum Mechanics of Many-Body Systems* (Academic, New York, 1972).

[36]We have assumed a nonrelativistic spin-independent Hamiltonian and considered the nuclei frozen at their equilibrium positions $\vec{R}_n$.

[37]See, e.g., Refs. 2 and 20.

[38]Implications of local gauge invariance have recently been revived: J. J. Forney, A. Quattropani, and F. Bassani, Nuovo Cimento B 37, 78 (1977); F. Bassani, J. J. Forney, and A. Quattropani, Phys. Rev. Lett. 39, 1070 (1977); D. H. Kobe, *ibid.* 40, 538 (1978); Am. J. Phys. 46, 342 (1978); Phys. Rev. A 19, 1876 (1979).

[39]J. C. Ward, Phys. Rev. 78, 182 (1950); Y. Takahashi, Nuovo Cimento 6, 371 (1957).

[40]cf. D. A. Kirzhnits, *Field Theoretical Methods in Many-Body Systems* (Pergamon, Oxford, 1967), Chap. 4.

[41]See, e.g., G. Wendin, *Structure and Bonding* (Springer, Heidelberg, 1981), Vol. 45, p. 1; see also A. Liebsch, Phys. Rev. Lett. 43, 1431 (1979).

[42]A. Sjölander and M. J. Stott, Phys. Rev. B 5, 2109 (1972).

[43]In the following we shall use the Bohr radius as the unit of length and the rydberg as the unit of energy ($\hbar=1$, $m=1/2$, $e^2=2$ in these units).

[44]D. L. Johnson, Phys. Rev. B 12, 3428 (1975).

[45]W. Kohn, Phys. Rev. B 7, 4388 (1973), and references therein.

[46]J. C. Slater and G. F. Koster, Phys. Rev. 94, 1498 (1954).

[47]A. Mauger and M. Lannoo, Phys. Rev. B 15, 2324 (1977).

[48]O. Jepsen and O. K. Andersen, Solid State Commun. 9, 1763 (1971); G. Lehmann and M. Taut, Phys. Status Solidi B 54, 469 (1972); J. Rath and A. J. Free man, Phys. Rev. B 11, 2109 (1975).

[49]See, e.g., Eq. (41) of J. Bernholc and S. T. Pantelides, Phys. Rev. B 18, 1780 (1978).

[50]A. Baldereschi, Phys. Rev. B 7, 5212 (1973); D. J. Chadi and M. L. Cohen, *ibid.* 8, 5747 (1973).

[51]R. M. Pick, M. H. Cohen, and R. M. Martin, Phys. Rev. B 1, 910 (1970).

[52]A. Bansil, Solid State Commun. 16, 885 (1975); R. Prasad and A. Bansil, Phys. Rev. B 21, 496 (1980), and references therein.

[53]M. H. Cohen and F. Keffer, Phys. Rev. 99, 1128 (1955).

[54]G. Srinivasan, Phys. Rev. 178, 1244 (1969).

[55]H. J. Mattausch, G. Strinati, and W. Hanke (unpublished).

[56]R. F. Egerton and M. J. Whelan, Philos. Mag. 30, 739 (1974).

[57]H. Raether, in *Springer Tracts in Modern Physics,* edited by G. Höhler (Springer, Berlin, 1965), Vol. 38, p. 84. The upward shift of the plasma resonance caused by the presence of the low-lying electron-hole continuum can be obtained also from a simplified theory. For instance, Eq. (8) of Hermanson's paper (Ref. 15) gives the shifted plasma frequency Ω_p in terms of the electron-gas plasma frequency ω_p and of the static dielectic constant ϵ_0 as $\Omega_p=\omega_p[\epsilon_0/(\epsilon_0-1)]^{1/2}$. In diamond where the experimental ϵ_0 is 5.85, one gets $\Omega_p=34.4$ eV.

[58]M. Ortuno and J. C. Inkson, J. Phys. C 12, 1065 (1979).

[59]M. C. Pease, *Methods of Matrix Algebra* (Academic, New York, 1965).

[60]W. C. Walker and J. Osantowski, Phys. Rev. 134, A153 (1964); C. D. Clark, P. J. Dean, and P. V. Harris, Proc. R. Soc. London, Ser. A 277, 312 (1964); P. J. Dean, E. C. Lightowlers, and D. R. Wight, Phys. Rev. 140, A352 (1965).

[61]P. Nozières and D. Pines, Phys. Rev. 111, 442 (1958);

see also Ref. 15.
[62]J. A. Alonso and M. P. Iniguez, Solid State Commun. 33, 59 (1980).
[63]F. J. Himpsel, J. A. Knapp, J. A. Van Vechten, and D. E. Eastman, Phys. Rev. B 20, 624 (1979).
[64]Correlation corrections were first treated within a local density approximation by J. E. Robinson, F. Bassani, R. S. Knox, and J. R. Schrieffer, Phys. Rev. Lett. 9, 215 (1962).
[65]S. T. Pantelides, Phys. Rev. B 11, 2391 (1975).
[66]E. O. Kane, Phys. Rev. B 4, 1910 (1971); J. F. Janak, A. R. Williams, and V. L. Moruzzi, *ibid.* 6, 4367 (1972); see also the first listing of Ref. 12.
[67]J. F. Janak, A. R. Williams, and V. L. Moruzzi, Phys. Rev. B 11, 1522 (1975).
[68]E. O. Kane, Phys. Rev. B 5, 1493 (1972).
[69]J. R. Chelikowsky and M. L. Cohen, Phys. Rev. B 10, 5095 (1974).
[70]L. Ley, M. Cardona, and R. A. Pollak, in *Photoemission in Solids II,* edited by L. Ley and M. Cardona (Springer, Berlin, 1979), p. 11.